Visakhapatnam Chapter

Proceedings of Indian Geotechnical Conference 2020
December 17-19, 2020, Andhra University, Visakhapatnam

Evaluation of Liquefaction Potential of Class F Fly Ash and Calibration of Numerical Model

Sangeeta Yadav[1] and Sumanta Haldar [2]

[1] M.Tech. Student, School of Infrastructure, IIT Bhubaneswar, India.
Email: sy15@iitbbs.ac.in
[2] Associate Professor, School of Infrastructure, IIT Bhubaneswar, India.
Email: sumanta@iitbbs.ac.in

Abstract. Due to the ever-increasing generation of fly ash in a large quantity, its disposal has become a huge problem all over the world. It can be utilized in large geotechnical earthworks without depleting the natural soil. Its use in the seismically active areas requires a profound understanding of its liquefaction behavior and generation of excess pore water pressure. In the present study, the liquefaction behavior of pond ash has been studied from the literature, which utilizes a series of Cyclic Triaxial tests on different pond ash samples. Results of the Cyclic Triaxial test available are calibrated using a two-dimensional finite element analysis Open System for Earthquake Engineering Simulation (*OpenSees*), and sensitivity analysis of the model parameters has been carried out. From the analysis, it is found that numerical results are in complacence with the experimental results and can be used as a reliable tool for the study of the earthquake-induced phenomenon.

Keywords: Fly ash, Cyclic Triaxial, Liquefaction potential, Calibration, Sensitivity.

1 Introduction

Fly ash is the finely divided residue that results from the combustion of pulverized coal. India has the fifth largest coal reserve in the world, and over 70% of the nation's power generation is coal-based. Globally 41% of electricity is produced from the thermal electric plants producing a considerable amount of fly ash, about which only 43% is used in cement, concrete, or brick manufacturing, and the rest is placed in the landfills. According to the Global Fly Ash Industry Analysis, fly ash production is expected to increase by 2.6 % by the year 2033, and production of 131 million tons of fly ash per year in the USA only. The plenitude of fly ash presents remarkable use in structural fills and other geotechnical applications. Since fly ash mainly consists of non-plastic silt size particles of relatively low permeability than sand, it is prone to liquefaction during earthquakes [1,9]. Hence it is essential to predict the liquefaction potential of the fly ash before using it in seismically active areas.

Jakka et al. [9] carried out a detailed study on liquefaction resistance of pond ash by conducting an undrained cyclic triaxial test and found that liquefaction resistance of pond ash varies significantly within the same pond from inflow to outflow point. The strength deformation behavior of the pond ash shows the relative density and the level of cyclic stress amplitude are the crucial parameters in the liquefaction potential of the pond ash, and its behavior is comparable with the granular soil containing 20% fines [4]. A similar observation is made by Kim and Prezzi [5] on class-F Indiana (US) fly ash. Observation made by Boominathan and Hari [1] and Vijayasri et al. [14] on reinforced pond ash shows good friction angle, better drainage properties, and improved liquefaction resistance of pond ash compared to the unreinforced ash material. It indicates that the pond ash, with reinforcement, can be used as an economical material in the seismic prone areas. Further liquefaction potential and post-liquefaction shear strength of impounded fly ash is reported by Zand et al. [3] and concluded that the liquefaction potential of fly ash is a stronger function of the initial dry density as well as low level effective confining stress as reported by Jakka et al. [9].

The performance of the structures with ash is influenced by several factors; hence it is important to carry out site-specific response studies. Jakka et al. [8] studied the performance of the ash embankments constructed by the upstream and downstream methods of construction to assess the suitability of ash as a geotechnical construction material. The influence of various factors on the dynamic properties of ash is investigated by Chattaraj and Sengupta, and correlations are proposed for predicting maximum Shear Modulus (G_{max}) and damping for the fly ash [7].

During the most recent couple of years, numerical investigations have too concentrated on the behavior of pond ash material under static and dynamic loadings. The effect of gradation on the dynamic response of pond ash has studied by Rahitya and Patra [11] using *OpenSees*. Vijayasari et al. [12,13] performed a two-dimensional dynamic response analysis using a fully coupled effective stress nonlinear approach on the Renusagar pond ash embankment in India, and the further extension of the study has focused on the mode shapes, fundamental period, acceleration intensification, horizontal and vertical displacement, nonlinear stress-strain behavior, cyclic stress ratio, and liquefaction potential. A similar study has been carried out on the Talcher pond ash embankment in India, considering the existing water table and full saturation condition [10].

It is evident that past studies mostly addressed the liquefaction potential of fly ash based experimental observation. However, limited studies have been carried out on the evaluation of the appropriate constitutive model for numerical analysis of the potentially liquefiable material. The constitutive model involves several material constants. Calibration of the model parameters is a time-consuming trial and error procedure; hence sensitivity analysis of the input parameters can be helpful to identify the relative importance of each parameter. This in turn helps to expedite the calibration process. In this study, the liquefaction triggering of the fly ash is simulated using nine node quadrilateral plane-strain elements with solid-fluid, fully coupled material that uses a pressure-dependent elastoplastic constitutive model in *OpenSees*.

2 Methodology

The present study adopted the test results of liquefaction potential assessment of class-F fly ash using stress-controlled cyclic triaxial tests from the literature [9]. The physical properties of pond ash are summarized in Table 1. The undrained cyclic triaxial test was conducted at an effective confining pressure of 106 kPa, cyclic stress ratio of 0.3, loading frequency of 0.1 Hz, and for the applied deviator stress, axial strain and excess pore water pressure were measured.

Table 1. physical properties of the fly ash [9]

Material properties	Value
Specific gravity	2.18
Initial Density (kN/m^3)	10.84
Coefficient of permeability (m/s)	9.4×10^{-7}
Friction angle (degrees)	37
Void ratio	0.97

2.1 Numerical model

Numerical models have proven to be an essential tool for solving practical problems. OpenSees is a software framework for simulation applications in earthquake engineering using Finite Element (FE) methods. The constitutive model, which can describe the essential features of the material behavior has been implemented in this FE model.

From geotechnical classification, the abovementioned pond ash is classified as silt; hence, *PressureDependentMultiYield02 (PDMY02)* material model for cohesionless soil is utilized for the numerical modeling. *PDMY02* is an elastic-plastic material for simulating the essential response characteristics of the pressure-sensitive material whose shear behavior is dependent on the confining pressure. To simulate the undrained behavior of pond ash, a solid-fluid fully coupled *u-p* element named *9_4_QuadUP* element is considered, and its configuration along with the boundary condition is shown in Fig.1.

It has 9 nodes for solid deformation (u) and 4 nodes for pore water pressure (p). Four corner nodes have three degrees of freedom (two translations and one pore water pressure), while the intermediate nodes have only two translational degrees of freedom. Base nodes are fixed in the horizontal and vertical directions, whereas the PWP degree of freedom is restricted for nodes 3 and 4.

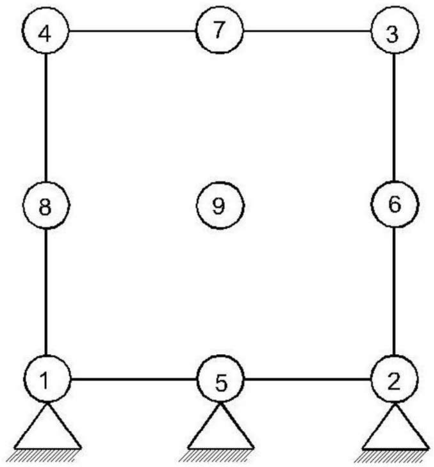

Fig. 1. Schematics of nine node solid-fluid fully coupled u-p element, 9_4_ QuadUP element

The loading is given in two stages. In the first stage, the hydrostatic condition is generated by incorporating gravity in the analysis, having a magnitude equal to the components of gravity in horizontal and vertical directions. In the second stage, cyclic loading is given by applying a sinusoidal wave of a particular frequency. Material behavior is considered to be linear elastic during the gravity loading stage, and in the subsequent loading phase, the stress-strain response is ensured plastic by updating the material stage. The formulation of plasticity is done using a multi-surface concept, and the Drucker-Prager yield surfaces are used. The flow rule is non- associative, in which the rate of plastic strain increment vector is not normal to the yield surface. For the numerical integration in the transient analysis, Newmark's integrator has been used with integration parameters gamma and beta as 0.6 and 0.3, respectively. The maximum number of iterations and tolerance is set as 50 and 10^{-3}, respectively.

PDMY02 model requires a total of 23 Parameters comprising 3 additional parameters namely Contrac2, Contrac3, and Dilate3. Some of the material parameters used in the model are shown in Table 2. Contrac1 defines the rate of contraction. Stronger is the contraction; larger is the reduction in effective vertical stress. Contrac2 is a constant reflecting dilation history on contraction tendency, stronger dilation results in a higher contraction in the subsequent unloading cycle. Dilate1 and Dilate2 reflect the rate of shear-induced dilation. Contrac3 and Dilate3 are the new parameters introduced in the model *PDMY02,* to account for the overburden stress effect. Parameters Liquefaction1 and Liquefaction2 are related to the accumulation of permanent shear strain as a function of dilation and load reversal history, respectively.

Pore water pressure, shear stresses, and shear strains are recorded using the *OpenSees* Element Recorder commands. The displacements and pore water pressure are recorded at the nodes. The stresses and strains are the most accurate at Gauss points; it is measured at different integration points instead of the nodes, thereafter, it is extrapolated to the rest of the element. The recorded outputs have been utilized for further analysis.

Table 2. Input parameters used in the model

Input parameters	Value	Remarks
Maximum shear modulus (kPa)	40000	-
Effective confining pressure (kPa)	106	-
Pressure dependent coefficient	0.5	-
Phase transformation angle (deg.)	27	-
Contrac1	0.013	Determines the shear-induced
Contrac2	5.0	decrease in volumetric strain to
Contrac3	0.1	develop pore water pressure.
Dilate1	0.2	Determines the shear-induced
Dilate2	3.0	increase in volumetric strain or
Dilate3	0.1	dilation

3 Results and Discussion

3.1 Model validation

Plots obtained from the result of finite element analysis are superimposed with that of the cyclic triaxial test performed by Jakka et al. [9]. The stress-strain response and the pore water pressure recorded is used for the validation of the numerical model. shows the typical stress-strain response, which matches reasonably well with the experimental result. *PDMY02* material model is capable of capturing many aspects of the soil response. In Fig. 3, pore water pressure is plotted in terms of excess pore pressure ratio with the number of cycles, and it is assumed that liquefaction is initiated at the point where excess pore pressure becomes almost equal to the initially applied confining pressure i.e. pore pressure ratio equals to one. Similar to the results reported by Jakka et al. [9], the finite element result shows that material reaches the state of initial liquefaction, and thereafter, pore pressure falls to the lower levels with the gradual development of strain exhibiting cyclic mobility type of liquefaction.

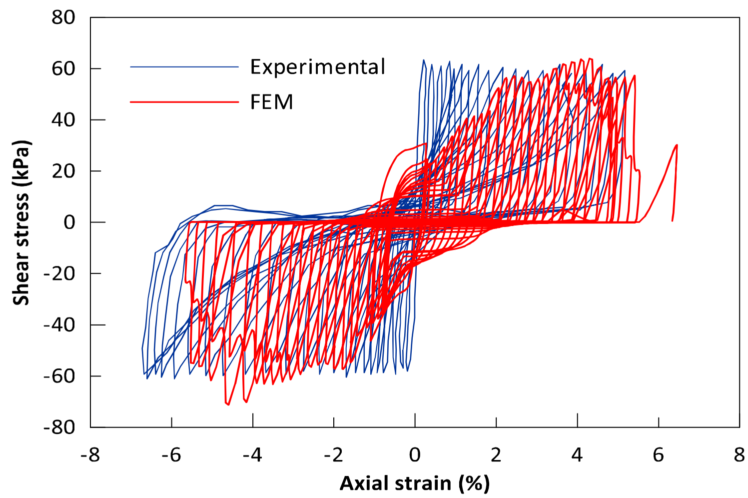

Fig. 2. Shear stress vs axial strain plot.

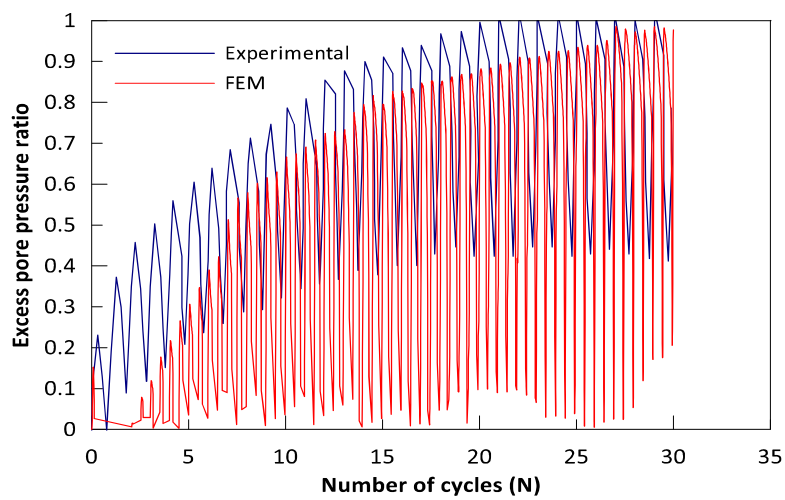

Fig. 3. Excess PWP ratio vs number of cycles

3.2 Sensitivity analysis

After calibration of the numerical model, sensitivity analysis is performed by varying only one parameter at a time and keeping the rest of the parameter constant. The result of sensitivity analysis is shown in Fig.4. The number of cycles required for initial liquefaction is considered as output. For the change in the input parameter, the corresponding change in output is recorded in percentage. A parameter that gives a higher slope is considered as sensitive. The recommended range of parameters for the *PDMY02* model can be found in the *OpenSees* manual [6].

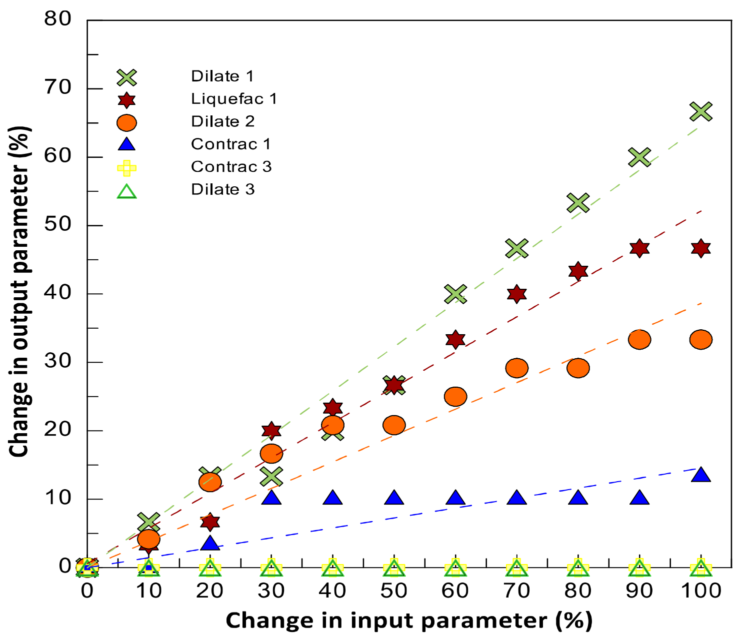

Fig.4. Sensitivity of input parameters

Contrac1 in the dense state is found marginal sensitive parameter; a 100% change in the input caused only a 13% change in the number of cycles. However, in a loose state, there is a significant change, which indicates the faster development of the PWP in the loose state as compared to the dense state. Fig 5 shows the effect of the Contrac1 parameter on the development of excess PWP. A small circle is used to indicate a point where liquefaction occurs (i.e., EPWPR = 1.0) for the different values of the input parameter. From Fig 5 it is clear that the higher contraction value results in faster volumetric reduction.

For the PDMY02 model, Contrac2 shall be fixed as 5, which represents a point where fabric damage is activated, at which, accumulated volumetric strain in the first dilation results in the more contractive behavior in the unloading cycle.

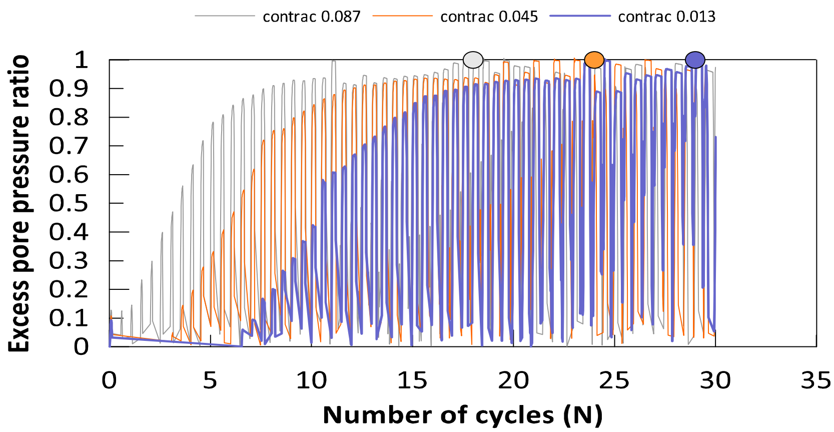

Fig. 5. Effect on Contraction1 parameter on excess PWP ratio.

From the sensitivity plot, Dilate1 is found to be the most sensitive. Fig (6) shows the effect of the Dilate1 parameter on the initiation of liquefaction. Even a small increase in the Dilate1 results in stronger dilation, as a result of which the material takes a greater number of cycles to get liquefied. Reduction in Dilate2 causes an increase in dilation; nonetheless, it is less sensitive than Dilation1. Khosravifar et al. [2] suggested to fix the Dilate2 parameter as constant; however, it can be varied between 3-0.3 for the soil specific calibration.

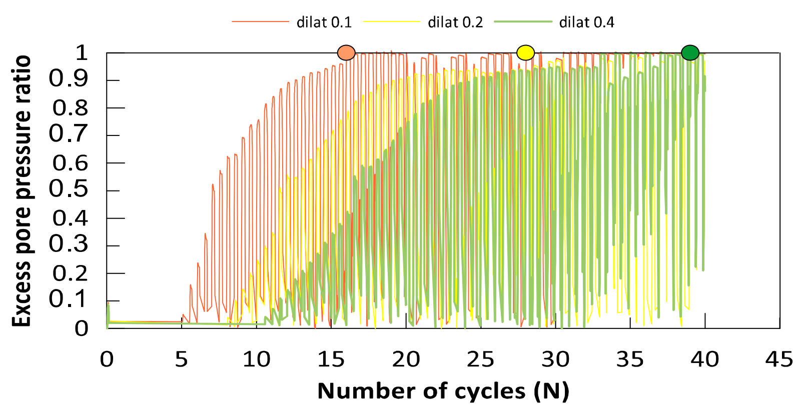

Fig. 6. Effect of Dilation1 parameter on Excess PWP ratio

For Contrac3, Dilate3, and Liquefaction2 within the range of 100%, no change is observed in the output; hence it can be called insensitive parameters. The liquefaction1 parameter has a significant effect on the development of excess PWP. It can be seen from fig 7 that the increase in this parameter results in the faster development of the excess PWP.

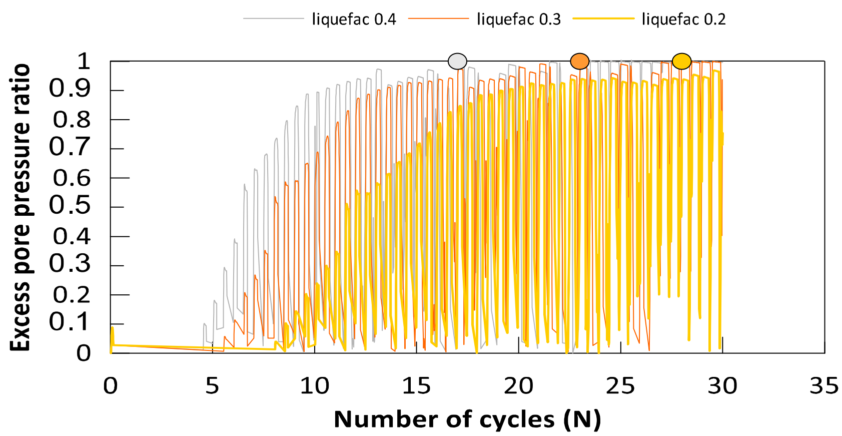

Fig. 7. Effect of Liquefaction1 on excess PWP ratio

4 Conclusions

From the above study carried out using a 2D finite element analysis, reasonably good agreement is found between the experimental and finite element results. Sensitivity analysis is also carried out to understand the trend of the input parameters used in the model. It can be concluded that Dilate1, Dilate2, Liquefac1 are the most sensitive, whereas Contrac3, Dilate3, and Liquefac2 are the least sensitive parameters. The sensitivity of parameters can vary depending upon the output selected for the analysis. Based on this study, calibration of a numerical model for the liquefaction triggering of fly-ash could be convenient with good computational efficiency. The critical assessment of the sensitivity will empower the geotechnical engineers in utilizing the numerical model with confidence in the evaluation of liquefaction induced deformation behavior of ash-dykes.

References

1. Boominathan, A., & Hari, S.: Liquefaction strength of fly ash reinforced with randomly distributed fibers. Soil Dynamics and Earthquake Engineering, 22(9-12), 1027-1033 (2002).
2. Khosravifar, A., Elgamal, A., Lu, J., & Li, J.: A 3D model for earthquake-induced liquefaction triggering and post-liquefaction response. Soil Dynamics and Earthquake Engineering, 110, 43-52 (2018).
3. Zand, B., Tu, W., Amaya, P. J., Wolfe, W. E., & Butalia, T. S.: An experimental investigation on liquefaction potential and post-liquefaction shear strength of impounded fly ash. Fuel, 88(7), 1160-1166 (2009).
4. Mohanty, B., Patra, N. R., & Chandra, S.: Cyclic triaxial behavior of pond ash. In GeoFlorida 2010: Advances in Analysis, Modeling & Design (pp. 833-841) (2010).
5. Kim, B., & Prezzi, M.: Evaluation of the mechanical properties of class-F fly ash. Waste management, 28(3), 649-659 (2008).
6. https://opensees.berkeley.edu/wiki/index.php/PressureDependMultiYield02_Material.
7. Chattaraj, R., & Sengupta, A.: Dynamic properties of fly ash. Journal of Materials in Civil Engineering, 29(1), 04016190 (2017).
8. Jakka, R. S., Ramana, G. V., & Datta, M.: Seismic slope stability of embankments constructed with pond ash. Geotechnical and Geological Engineering, 29(5), 821-835 (2011).
9. Jakka, R. S., Datta, M., & Ramana, G. V.: Liquefaction behavior of loose and compacted pond ash. Soil Dynamics and Earthquake Engineering, 30(7), 580-590 (2010).
10. Mohanty, S., & Patra, N. R.: Dynamic response analysis of Talcher pond ash embankment in India. Soil Dynamics and Earthquake Engineering, 84, 238-250 (2016).
11. Rahitya, S., & Patra, N. R.: Effect of gradation on dynamic response of pond ash embankment.
12. Vijayasri, T., Raychowdhury, P., & Patra, N. R.: Numerical simulation of the dynamic behavior of Renusagar pond ash embankment in India using a fully coupled nonlinear approach. Discovery, 40, 20-26 (2015).
13. Vijayasri, T., Raychowdhury, P., & Patra, N. R.: Seismic response analysis of Renusagar pond ash embankment in Northern India. International Journal of Geomechanics, 17(6), 04016141 (2017).
14. Vijayasri, T., Patra, N. R., & Raychowdhury, P.: Cyclic behavior and liquefaction potential of Renusagar pond ash reinforced with geotextiles. Journal of Materials in Civil Engineering, 28(11), 04016125 (2016).